

EARTH PRESSURE ON RETAINING WALLS NEAR ROCK FACES

By Sam Frydman¹ and Israel Keissar²

ABSTRACT: The present study examines the lateral earth pressure transferred to a rigid retaining wall by granular fill confined between the wall and an adjacent rock face. The centrifuge modeling technique is used to test small models in which rotation of the wall about its base can be controlled, thus allowing observation of changes in pressure from the at-rest to the active condition. Janssen's silo pressure equation may be reasonably used for estimation of the at-rest pressure, using an earth pressure coefficient, $K = 1 - \sin \Phi$. Significant variations from the estimated pressure may occur next to the wall as a result of small variations in placement conditions. A conservative approach may be to use a decreased Φ value in calculating K . In the active condition, progressive failure in the soil results in a decreased Φ , which should be used when estimating wall pressure. These estimates may be obtained from stress characteristic solutions, or from the silo pressure equation in which a K value compatible with the values of Φ and δ (wall friction angle) is used.

INTRODUCTION

The estimation of lateral earth pressure acting on a retaining wall built close to a stable rock face, with granular fill placed between them, such as that shown schematically in Fig. 1, has received very little attention in the literature. The fill is partly supported by friction on the wall and the rock face; consequently, the vertical stress in the fill and the horizontal stress acting on the wall are reduced. The design of these walls using Rankine pressure distribution or Coulomb lateral force coefficients (e.g., Ref. 7) may be expected to be overly conservative. One approach, suggested by Spangler and Handy (14), is to estimate the lateral stress distribution using Eq. 1, which is based on Janssen's arching theory (5) and is commonly used for calculating silo pressure:

$$\sigma_x = \frac{\gamma b}{2 \tan \delta} \left[1 - \exp \left(-2K \frac{z}{b} \tan \delta \right) \right] \dots \dots \dots \quad (1)$$

where b = the distance between the walls; z = depth from wall top at which σ_x is required; K = the coefficient of lateral earth pressure; γ = the unit weight of the fill; and δ = the angle of friction between the "walls" and the fill.

Spangler and Handy do not discuss the choice of the value of K to be used in the calculation, although they show an example calculation in which the Rankine active coefficient, K_a , is used. Handy (4) suggests the use of a coefficient K_w , which is related to Φ and σ_2 as described

¹Assoc. Prof., Faculty of Civ. Engrg., Technion—Israel Inst. of Tech., Technion City, Haifa 32000, Israel.

²Res. Student, Faculty of Civ. Engrg., Technion—Israel Inst. of Tech., Technion City, Haifa 32000, Israel.

Note.—Discussion open until November 1, 1987. To extend the closing date one month, a written request must be filed with the ASCE Manager of Journals. The manuscript for this paper was submitted for review and possible publication on May 20, 1986. This paper is part of the *Journal of Geotechnical Engineering*, Vol. 113, No. 6, June, 1987. ©ASCE, ISSN 0733-9410/87/0006-0586/\$01.00. Paper No. 21544.

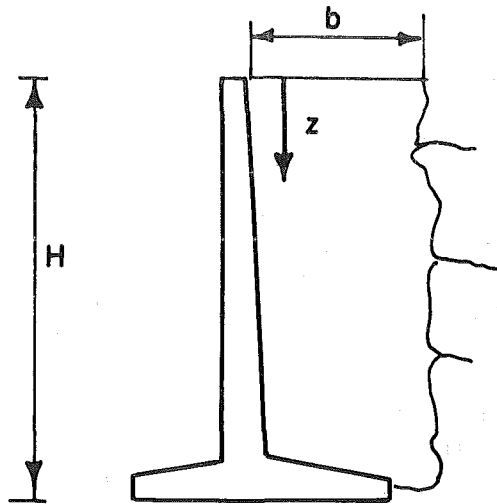


FIG. 1.—Schematic Representation of Retaining Wall near Rock Face

later. There would appear to be a case for assuming the K -value to be related to the state of movement of the wall. It may at first seem reasonable to assume K_0 for no wall movement, and K_a if the wall moves sufficiently to induce active failure conditions in the fill.

Another obvious problem associated with the use of Eq. 1 is that it requires adoption of a single value of δ between both walls (i.e., the wall and the rock face, in the present case) and the fill. In the present case, different values of δ could exist along the wall and the rock face, and so an average value would need to be used.

For the active case, an alternative approach, which can take account of the different δ values, is to develop a statically admissible stress field in the fill, which is based on slip lines (stress characteristics). As was pointed out by Frydman and Baker (3), stress characteristics would be expected to correspond to slip lines in the present active case, as compared to the passive case, in which velocity characteristics would correspond to slip lines.

Despite the availability of the preceding techniques for estimating lateral pressure on walls adjacent to rock faces, their confident application requires some satisfactory verification from measurements on models or full-scale prototypes. To the writers' knowledge, no measurements on full-scale or model walls of the foregoing type have been reported. This paper presents a study of the lateral pressures acting on such walls.

MODELS AND TESTING SCHEME

The use of small-scale models for the study of active earth pressure problems is difficult due to the very small magnitude of the lateral stresses that are to be measured. In the case of fill of limited extent behind the

wall, which is discussed here, this difficulty would be expected to be magnified, in view of the expected decrease in these stresses. In addition to these difficulties, it is now well accepted (e.g., Ref. 2) that small-scale models can lead to quite erroneous conclusions regarding soil-structure interaction effects. Handy (4) compared measured values of earth pressures on three retaining walls of different heights to values predicted on the basis of arching theory. He concluded that "the difference in behaviour of the three wall heights carries an interesting implication with regard to modeling: That, since the soil stress-strain behaviour cannot be scaled, experimentation should ideally be at full scale."

Both of these problems can be solved by centrifuge modeling, whereby similitude is upheld and model stresses are of prototype level. This technique is used for the present study.

Centrifuge.—The centrifuge system employed has been described elsewhere (8). It has a mean radius of 1.5 m, can develop a maximum acceleration of 100 g, where g is acceleration due to gravity, and carry a maximum payload of 5,000 kg-gravities. Fifteen slip rings are available for transfer of electric signals. The model may be photographed in spin using a short duration stroboscope flash triggered by a reed relay system.

Models.—The models are built in an aluminum box of inside dimensions 327 × 210 × 100 mm, as shown in Figs. 2(a–c). Each model in-

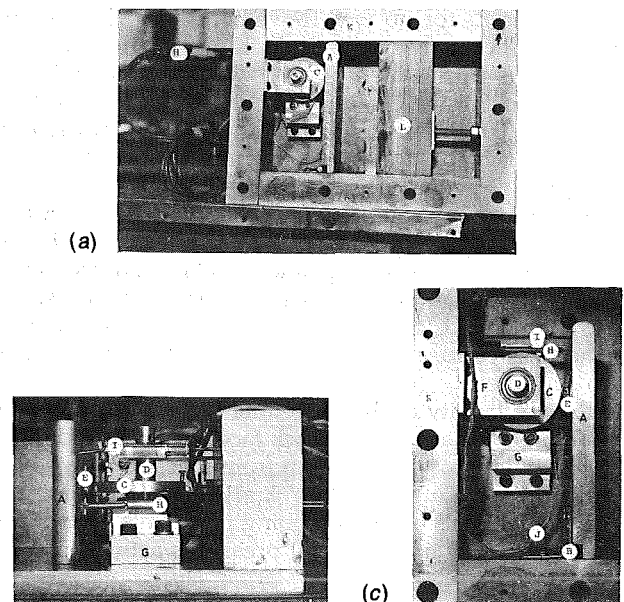


FIG. 2.—Model: (a) General Side View; (b) Movement Control System Top View; (c) Movement Control System, Side View (Legend: A = Retaining Wall; B = Hinge; C = Eccentric Disk; D = Motor Axis; E = Bushing; F = Motor Axis Support; G = Motor Support; H = LVDT; I = Spring; J = Electric Wires from Pressure Cells; K = Model Box; L = Wooden Simulation Rock Face)

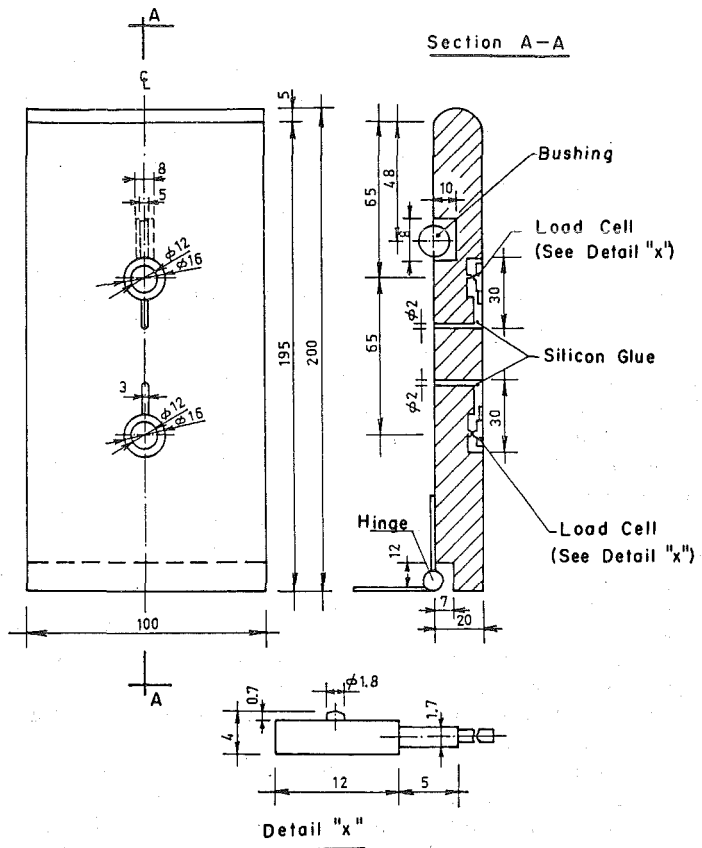


FIG. 3.—Model Retaining Wall

cludes a retaining wall made from aluminum (195 mm high \times 100 mm wide \times 20 mm thick) connected to the base of the box by a hinge, allowing rotation of the wall about its base. The back of the wall is supported by a disk, eccentrically mounted on the axis of an electric step motor; movement of the wall is controlled by rotation of the disk and measured by a LVDT. Contact between the disk and the wall is through a bushing, thus minimizing friction. Two load cells (Kyowa, LM-A series; see Fig. 3) are inset flush with the wall face, at 1/3 and 2/3 of wall height. The rockface is modeled by a wooden block, which can, through a screw arrangement, be positioned at varying distances from the wall. The face of the block is coated with the sand used as fill, so that the friction between the rock face and the fill is equal to the angle of internal friction of the fill.

Rotation of the wall is affected by the electric motor-disk system. The motor receives current in pulses of 1/10 sec duration; each pulse rotates the axis by about 1°. The aluminum disk (70 mm diameter) is mounted on the axis with an eccentricity of 5 mm. During setup of the model,

the wall is vertical and the disk is aligned so that the distance between the wall and the axis is a maximum. During placement of the fill and run-up of the centrifuge, movement of the wall is prevented by the support of the disk. Controlled wall rotation is allowed during centrifuge spin by applying a programmed number of pulses from a press button controller in the control room. As a result of the 1° rotation of the disk accompanying each pulse, the disk contact moves away from the wall, and the wall, with the fill pressure on it, follows. The movement is monitored by the LVDT. In view of the fact that a wall top movement of the order of 0.1% of its height is expected to result in development of active conditions in the fill (10), a movement of about 0.2 mm would be required for the 195 mm model walls. The present system develops this movement with about 20 pulses, making it possible to study the transition from the "at-rest" to the active condition.

Model Fill.—The granular fill between the wall and the rock face was modeled by uniform fine sand from the Haifa Bay area. Particle size is in the range of 0.1–0.3 mm, and the uniformity coefficient, $C_u = 1.5$. Maximum density = 16.4 kN/m^3 and minimum density = 14.0 kN/m^3 . The model tests were carried out with the sand placed at a relative density of 70%; simple shear tests performed on the sand at this relative density gave values of the angle of internal friction $\Phi = 36^\circ$. Direct shear tests between the sand and aluminum yielded a value of 20° – 25° .

Calibration of Load Cells.—When pressure or load cells are used to measure pressures acting in soil, arching in the soil next to the cell face may lead to over- or under-registration of the cell; this effect is called "cell action" (9,17) and must be accounted for in the calibration of the cell. This is done by covering the cell face with a layer of the soil and applying the pressure over the top of the layer (17). In the present study, the load cells were calibrated using two different procedures, following their installation in the model walls. In both cases, the wall was placed, load cell face upwards, on the bottom of the model box and covered with a layer of sand at the required density. In the first procedure, pressure was applied to the face of the sand through an air bag; in the second, the model box was placed in the centrifuge and run up to 50 g with the centrifugal force normal to the load cell face. Excellent agreement was obtained between the two procedures, as shown in Fig. 4, which shows calibration curves for one of the cells. The calibration obtained using air pressure without a cover layer of sand is also shown. The air pressure calibration is seen to lie above that obtained when a soil layer covers the cell; this is in agreement with the findings of others (e.g., Ref. 17). Several repetitions of the calibration procedures indicated little scatter and very little effect of sand density on the calibration curves; the maximum range for repeated tests, at relative densities of 70% and about 0%, was 10%. This is within the accuracy range suggested by Trollope and Lee (17) to be obtainable at a measuring point at a sand boundary.

The hysteretic nature of the calibration curve raises the question as to which curve is the relevant one for the problem under study. Although it may appear, at first sight, that the unloading curve should be used for the active earth pressure case, consideration of the source of the hysteresis indicates that this is not so. When load is applied to a soil element

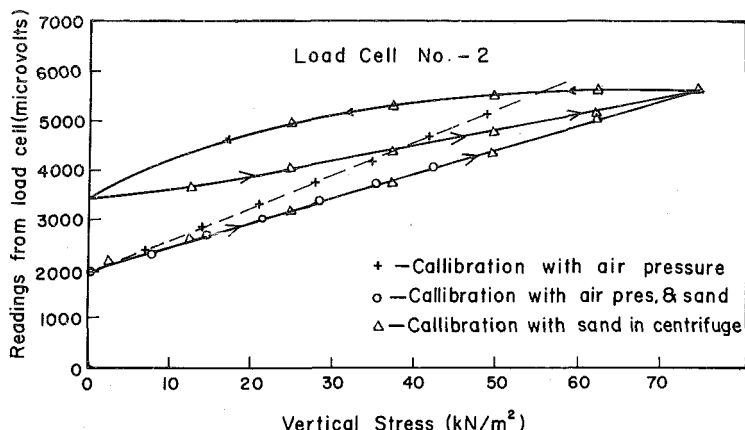


FIG. 4.—Typical Calibration Curves for Load Cells

in contact with a pressure cell face, the element pushes against the cell. The movement of the element is a function of the flexibility of the cell and the stiffness of the soil. During this process, plastic strains develop in the soil, so that when the load is released, and the cell-wall face is not moved, the cell, which is elastics, rebounds more than the plastic soil, pushes against the soil and over-registration of the cell results. Clearly, in cases where externally applied load is being reduced next to a fixed pressure cell, measurements should be interpreted using the unload calibration curve. In the case of active conditions, however, the cell is moving away from the soil, and thus there is no cause for overregistration.

Effect of Side Friction.—Bransby and Smith (1) considered the effect of side friction in model retaining wall experiments. They demonstrated that the effect may be very significant in passive pressure problems, but of little significance in active pressure problems. For sand with $\Phi = 35^\circ$ and a friction angle $\delta = 30^\circ$ between the sand and the model sides, they found that the decrease in measured K_a would be less than 14%.

In the present study, the sand fill is confined between an aluminum plate on one side and a glass plate on the other. Direct shear tests showed values of $\delta = 20^\circ\text{--}25^\circ$ between the sand and aluminum, and $\delta = 12^\circ\text{--}15^\circ$ between the sand and the glass. The effect of side friction may therefore be assumed to be small in the present investigation.

Preparation Compaction Stresses.—The models were prepared by compacting the dry sand in three layers to a relative density of 70%. As a result of this preparation technique, residual compaction-induced earth pressures acted on the wall following the completion of compaction. Obviously, these pressures would be expected to bear little resemblance to those that would develop as a result of field placement and their existence in conventional small-scale models, tested at 1 g, would lead to serious difficulties in interpretation of test results. This, in fact, is a further difficulty associated with the testing of small-scale models, where such placement effects may overshadow those of other processes that

are being studied. In centrifuged models, the significance of the residual compaction-induced earth pressures decreases as the g level increases; in the present investigation, their effect disappears at g levels of greater than about 10–15 g , where lateral pressure applied due to soil weight exceeds the residual compaction values. This phenomenon is discussed by Leschinsky, et al. (8). By testing the models at g levels above 10–15 g , measured lateral pressures are those resulting from soil weight; if it were desired to study compaction-induced earth pressures, a simulation of the field compaction procedure should be applied to the model under its raised g level.

ESTIMATED AND MEASURED PRESSURE DISTRIBUTIONS

Defining modified earth pressure coefficients, K'_0 and K'_a , as the ratio σ_x/σ_z relevant to at-rest and active conditions, respectively, Janssen's arching theory, as expressed by Eq. 1, with K taken as K_0 or K_a leads to

$$K'_0 = \frac{1}{2 \tan \delta z} \left[1 - \exp \left(-2 K_0 \frac{z}{b} \tan \delta \right) \right] \dots \dots \dots \quad (2a)$$

$$K'_a = \frac{1}{2 \tan \delta z} \left[1 - \exp \left(-2 K_a \frac{z}{b} \tan \delta \right) \right] \dots \dots \dots \quad (2b)$$

Figs. 5(a-b) show the dependence of K'_0 and K'_a on the ratio z/b for a number of combinations of Φ and δ . The term K_a used in Eq. 2 is obtained from Rankine's expression $(1 - \sin \Phi)/(1 + \sin \Phi)$; K_0 is obtained from the empirical approximation $(1 - \sin \Phi)$. It is appreciated that, in fact, the value of δ will vary both with rotation of the wall and with location along the wall. In estimating lateral pressure, it is convenient to assume δ constant and this assumption is employed herein.

Figs. 6(a–b) show stress characteristic fields (13) for two limiting cases of wall friction. Fig. 6(a) is for a wall friction angle, δ , of 25° , while Fig.

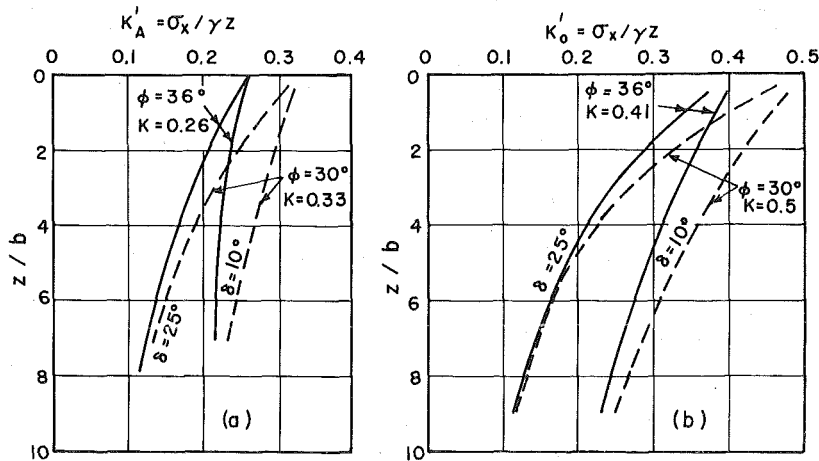


FIG. 5.—Dependence of (a) K'_u ; (b) K'_g on z/b , from Silo Pressure Equation

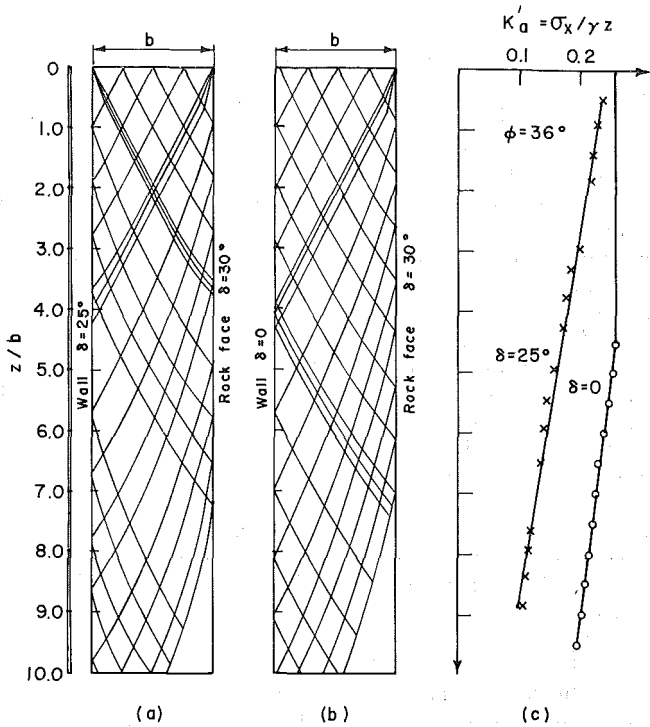


FIG. 6.—Stress Characteristic Solutions

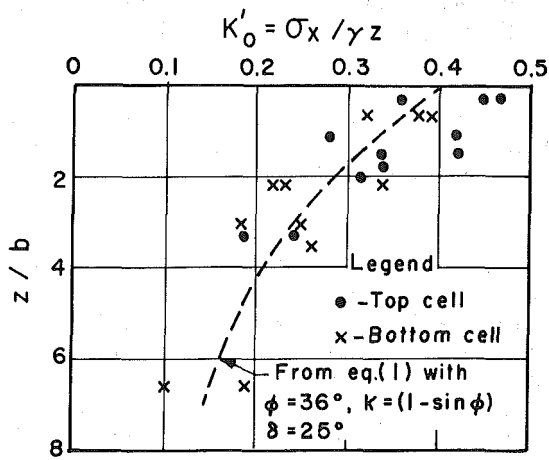


FIG. 7.—Measured and Calculated Values of K'_0 , versus z/b

6(b) is for $\delta = 0$. In both cases, Φ has been taken as 36° , and the friction angle on the rock face as 30° . Fig. 6(c) shows the distribution of K'_n along the wall, as obtained from the stress field analysis.

Tests were run on models with ratios of b/H (ratio of width of fill to wall height) = 1.1, 0.3, 0.22, 0.19, and 0.1. In each test, the model was spun up to an initial acceleration condition corresponding to 43.7 g at the midheight of the wall, without any wall movement. Load cell readings taken at this stage yielded values of at-rest pressure and, consequently, of K'_0 . The wall was then allowed to rotate about its base while load cell measurements were taken. The stress levels developed in these models would be similar to those next to full-scale walls having a height of about 8.5 m.

At-Rest Condition.—Fig. 7 shows the measured values of K'_0 as a function of z/b ; the theoretical silo pressure curve for $\Phi = 36^\circ$ and $\delta = 25^\circ$ is superimposed on the figure. The theoretical curve is seen to show fair agreement with the experimental points, although considerable scatter is evident, reflecting the sensitivity of at-rest pressure measurements to slight variations in placement conditions and local density variations (17). It would appear reasonable to use Eq. 2 for estimation of at-rest pressure.

Active Condition.—Fig. 8 shows the transition of K' from the at-rest to the active condition in some of the tests. The overall pattern observed in the tests is that for cases in which K'_0 is greater than about 0.25, where K' decreases in the transition. When K'_0 is less than about 0.25, K' increases towards the active condition.

Noting that the value $K' = 0.25$ is close to the Rankine active pressure coefficient of the sand, it is suggested that the increase in K' for initially lower values results from partial breakdown of the arching mechanism during movement of the wall. The fact that arching within a granular mass degenerates as a result of such movement is discussed by Rowe (8) to explain redistribution of active pressure on an anchored sheet pile wall in which the anchor yields. Terzaghi (11), introducing his classical presentation of the subject of arching, warned that

every external influence which causes a supplementary settlement of a footing or an additional outward movement of a retaining wall under unchanged static forces must also be expected to reduce the intensity of existing arching effects.

In the present case, when rotation of the wall occurs, some of the arching associated with the at-rest condition of the wall is reduced. The at-rest pressure is higher than the Rankine active pressure, which would develop on rotation of the wall even if all the arching were destroyed, then K' decreases when the soil is transferred from the at-rest to the active state. However, when, as a result of significant arching, the at-rest pressure is low compared to the Rankine active pressure, a pressure increase may occur during wall rotation, as arching is reduced and K' tends towards the Rankine value.

Some deviations are evident in the shapes and relative locations of the curves in Fig. 8; the two curves for $z/b = 3$ and 3.3 are an example. These curves would be expected to be similar but appear to be basically

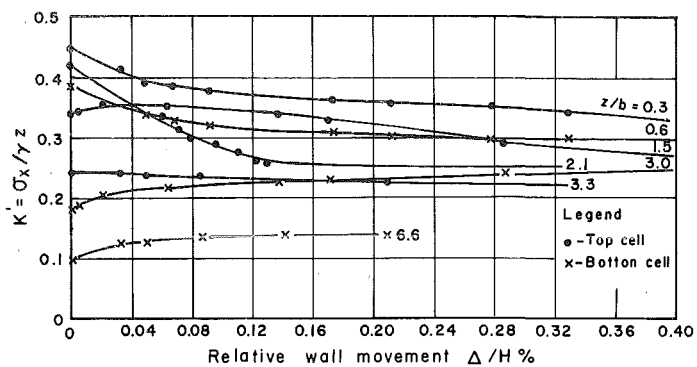


FIG. 8.—Transition of K' from At-Rest to Active Condition

different; the former indicates an increase in K' during transition from at-rest to active conditions and the latter indicates a decrease. In fact, the K'_0 values in the two tests were 0.185 and 0.24, the difference presumably being due to slight differences in placement conditions. Despite this difference, both models developed similar values of K'_a (0.25 and 0.225, respectively), indicating the lesser effect of a slight difference in placement conditions on active, rather than at-rest, pressures.

Fig. 9 shows the experimental variation of K'_a with z/b , together with theoretical silo pressure curves for $\Phi = 36^\circ$ and $\delta = 25^\circ$ and 20° . In this case, the theoretical curves clearly underestimate the measured values. Underestimation also results from use of the stress characteristic solution, as seen in Fig. 10, which shows the pressure distribution for $\Phi = 36^\circ$ and $\delta = 25^\circ$ on the wall and 30° on the excavation face.

The fact that measured lateral pressures considerably exceed estimated values under active conditions may be a result of progressive failure in the sand mass adjacent to the rotating wall, due to the fact that failure is reached at different stages at different points in the mass. This phenomenon has been observed for the case of walls under passive con-

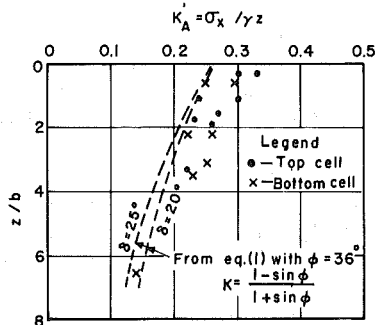


FIG. 9.—Comparison between K'_a Measured and Calculated from Silo Pressure Equation

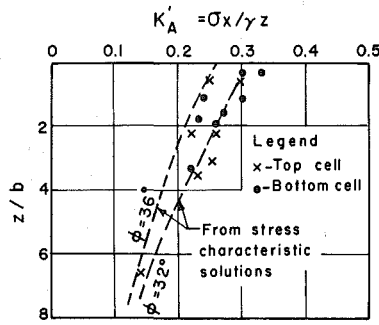


FIG. 10.—Comparison between K'_a Measured and Calculated from Stress Characteristic Solution

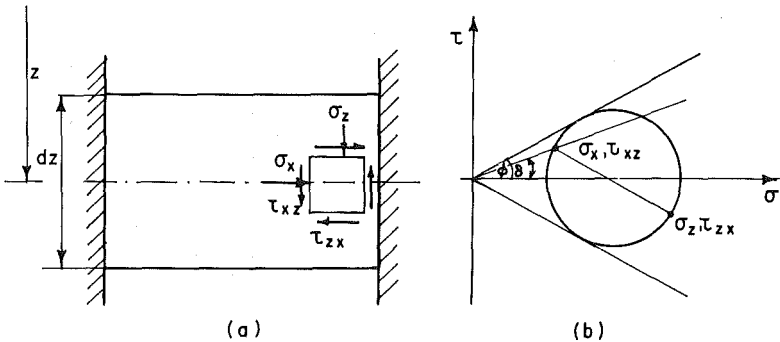


FIG. 11.—Stress Conditions Adjacent to Retaining Wall

ditions (e.g., Refs. 6 and 11), and for walls under active conditions and bearing capacity problems (12), where the mean mobilized Φ value in the rupture zone of dense sand fill, Φ_m , is between Φ_{\max} and Φ_{cv} . A stress characteristic pressure distribution, obtained by assuming $\Phi = 32^\circ$, is superimposed on Fig. 10. It is seen that most of the experimental points are enclosed by the two curves corresponding to $\Phi = 36^\circ$ and 32° . The use of the silo pressure equation may similarly be improved by using a decreased value of Φ . In addition, further consideration is given here to the K value that should most reasonably be used in applying Eq. 1 to the present problem. Fig. 11(a) shows a horizontal strip of soil located between two vertical surfaces on which the friction angle is δ . In view of the fact that an active wall is being considered, it is reasonable to assume that the soil is in a state of failure. Fig. 11(b) shows the Mohr circle of stress for element A adjacent to the wall. From trigonometry, it can be shown that the ratio $K = \sigma_x/\sigma_z$ is given by

$$K = \frac{(\sin^2 \Phi + 1) - \sqrt{(\sin^2 \Phi + 1)^2 - (1 - \sin^2 \Phi)(4 \tan^2 \delta - \sin^2 \Phi + 1)}}{(4 \tan^2 \delta - \sin^2 \Phi + 1)} \dots \dots \dots (3)$$

Eq. 3 indicates that K is a function of Φ and δ ; the variation of K with Φ for different values of δ is shown in Fig. 12. Handy (4), who also considered this problem, suggested the use of $K_w = \sigma_x/(\sigma_z)_{av}$, where $(\sigma_z)_{av} =$ the average vertical stress across the soil section at the depth under consideration. Using Handy's analysis, it is found that σ_z and $(\sigma_z)_{av}$ are expected to differ by less than 10% and so the K -values suggested by the two approaches are similar.

For any pair of values Φ , δ , Eq. 2 may now be used with a value of K obtained from Eq. 3 or Fig. 12, to obtain a distribution of K'_a as a function of z/b . Such a distribution is shown in Fig. 13 for $\Phi = 36^\circ$ and $\delta = 25^\circ$; also shown is the Rankine value of $K_a = 0.26$, corresponding to $\delta = 0$. It is seen that for z/b less than about 1, the horizontal stress estimated using the silo pressure equation is greater than that corresponding to Rankine distribution. Obviously this is unacceptable, indicating the inapplicability of the silo analogy to the top of the wall. In this zone, where stress levels are small, the errors introduced by the simplifying assumptions of the model (e.g., that vertical pressure on any horizontal section

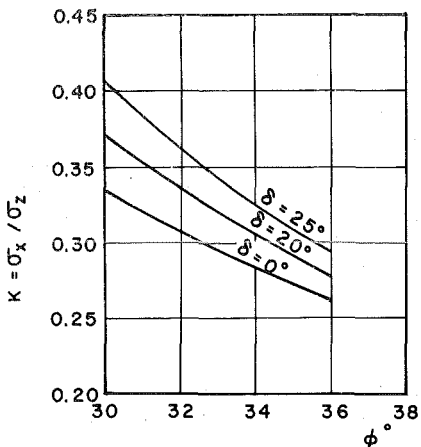


FIG. 12.—Lateral Earth Pressure Coefficient $K = \sigma_x/\sigma_z$ as Function of δ and Φ

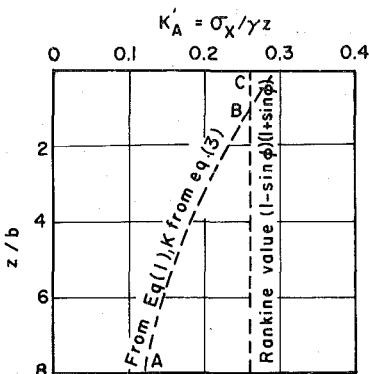


FIG. 13.—Distribution of K'_a with z/b , from Silo Pressure Equation, Using K from Eq. 3

through the fill is uniformly distributed) are likely to be more significant. A more reasonable distribution may be obtained by assuming the silo pressure curve to be limited by the Rankine pressure, resulting in a composite curve such as ABC in Fig. 13. Curves of this type have been drawn for $\Phi = 36^\circ$ and $\delta = 25^\circ$ and for $\Phi = 32^\circ$ and $\delta = 25^\circ$; these are shown in Fig. 14 together with pressure distributions obtained from stress characteristic solutions for $\Phi = 36^\circ$ and 32° with $\delta = 25^\circ$ on the wall and 30° on the rock face. Good agreement is observed between the two calcu-

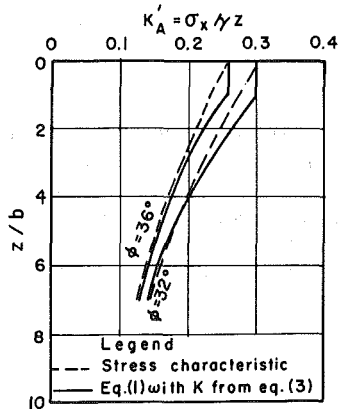


FIG. 14.—Comparison between K'_a Distributions Obtained from Silo Pressure Equation Using K from Eq. 3 and from Stress Characteristic Solution

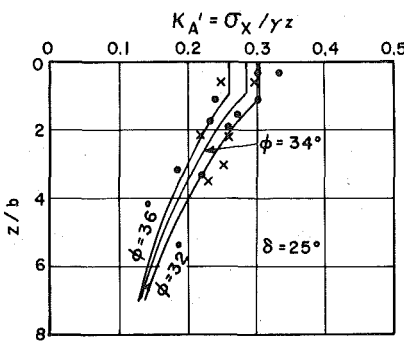


FIG. 15.—Comparison between K'_a Distributions Obtained from Silo Pressure Equation Using K from Eq. 3 and Measured Values

lation methods; the silo pressure curves are slightly higher at small ratios of z/b .

Fig. 15 shows silo pressure distributions for K obtained from Eq. 3, superimposed on the measured pressure values. The curves for $\Phi = 36^\circ$ and $\delta = 32^\circ$ are seen to reasonably include the results.

From an examination of Figs. 10 and 15, it appears that a calculation based on both the stress characteristic solution and the silo pressure equation may be used to estimate the lateral pressure distribution on the wall, as long as suitable Φ values are employed. In practice, the use of the silo pressure equation is much simpler.

CONCLUSIONS

The results of a study of the lateral pressure transferred to a rigid retaining wall by granular fill confined between the wall and an adjacent rock face are presented. It is found that Eq. 1, commonly used for estimating lateral pressure on silo walls, may be used to calculate the pressure for the no-movement (K_0) condition, using a K value of $1 - \sin \Phi$. Significant variations from the estimated pressure value may occur next to the wall, due to small variations in placement conditions (e.g., localized compaction effects, slight variations in density, etc.). A conservative approach could be to use a decreased Φ value in calculating K , so as to obtain an upper envelope to the expected pressure values.

The pressures acting on the wall, when it reaches an active condition by rotating about its base, appears to be less sensitive to small variations in placement conditions. Progressive failure, which occurs within the soil mass adjacent to the wall during its rotation, results in a decrease in Φ , and this decreased value must be used in estimating the pressure acting on the wall. Reasonable estimates of wall pressure may be obtained either from a stress characteristic solution, or from application of the silo pressure equation, in which a K -value compatible with the values of Φ and δ (see Eq. 3) is used.

ACKNOWLEDGMENTS

The study described in this paper was partially financed by the Israel Ministry of Housing and Development. The encouragement and cooperation of M. Sokolovsky, chief soils engineer of the ministry, is appreciated. The centrifuge employed in the investigation belongs to the Israel Defence Ministry. The writers appreciate the cooperation and assistance of the centrifuge technical staff, and of S. Samuel, Technion technician, for his technical assistance throughout the study.

APPENDIX.—REFERENCES

1. Bransby, P. L., and Smith, I. A. A., "Side Friction in Model Retaining Wall Experiments," *Journal of the Geotechnical Engineering Division*, ASCE, Vol. 101, No. 7, Jul., 1975, pp. 615–632.
2. Frydman, S., "Soil Structure Interaction," *State-of-the-Art Volume on Geotechnical Centrifuge Modelling*, 11th International Conference on Soil Mechanics and Foundation Engineering, San Francisco, Calif., 1985.

3. Frydman, S., and Baker, R., "On the Solution of Plane Strain Problems for Non-Associative Soils," *Proceedings*, IUTAM Conference on Deformation and Failure of Granular Materials, Delft, Holland, 1982, pp. 535-544.
4. Handy, R. L., "The Arch in Soil Arching," *Journal of Geotechnical Engineering*, ASCE, Vol. 111, No. 3, Mar., 1985, pp. 302-318.
5. Janssen, H. A., "Versuche über Getreidedruck in Silozellen," *Zeitschrift, Verein Deutscher Ingenieure*, Vol. 39, 1895, pp. 1045-1049. Partial English Translation in *Proceedings of Institute of Civil Engineers*, London, England, 1896, p. 553.
6. Kerisel, J., "The Language of Models in Soil Mechanics," *Proceedings*, 5th European Conference on Soil Mechanics and Foundation Engineering, Vol. 2, Madrid, Spain, 1972, pp. 9-30.
7. Kezdi, A., "Lateral Earth Pressure," *Foundation Engineering Handbook*, H. G. Winterkorn and H.-Y. Fang, Eds., Van Nostrand Rheinhold Co., New York, N.Y., 1974.
8. Leschinsky, D., Frydman, S., and Baker, R., "Study of Soil Structure Interaction Using Finite Elements and Centrifugal Models," *Canadian Geotechnical Journal*, Vol. 18, 1981, pp. 345-359.
9. Morgan, J. R., and Moore, P. J., "Experimental Techniques," *Soil Mechanics, Selected Topics*, I. K. Lee, Ed., Butterworth, London, England, 1968, pp. 295-340.
10. Rowe, P. W., "Anchored Sheet-Pile Walls," *Proceedings*, Institute of Civil Engineers, Vol. 1, Part 1, London, England, 1952, pp. 27-70.
11. Rowe, P. W., and Peaker, K., "Passive Earth Pressure Measurements," *Geotechnique*, Vol. 15, No. 1, 1965, pp. 22-52.
12. Rowe, P. W., "Progressive Failure and Strength of a Sand Mass," *Proceedings*, 7th International Conference on Soil Mechanics and Foundation Engineering, Vol. 1, pp. 341-349.
13. Sokolovski, V. V., *Statics of Soil Media*, Butterworths Scientific Publications, London, England, 1960.
14. Spangler, M. G., and Handy, R. L., *Soil Engineering*, Harper and Row, New York, N.Y., 1984.
15. Terzaghi, K., *Theoretical Soil Mechanics*, John Wiley and Sons, Inc., New York, N.Y., 1943.
16. Terzaghi, K., "Anchored Bulkheads," *Transactions*, ASCE, Vol. 119, 1954, pp. 1243-1324.
17. Trollope, D. H., and Lee, I. K., "The Measurement of Soil Pressures," *Proceedings*, 5th International Conference on Soil Mechanics and Foundation Engineering, Vol. 2, pp. 493-499.